iJRASET
International Journal For Research in Applied Science and Engineering Technology

INTERNATIONAL JOURNAL FOR RESEARCH

IN APPLIED SCIENCE & ENGINEERING TECHNOLOGY

Volume: 6 **Issue:** IV **Month of publication:** April 2018

DOI: http://doi.org/10.22214/ijraset.2018.4603

www.ijraset.com

Call: 08813907089 | E-mail ID: ijraset@gmail.com

International Journal for Research in Applied Science & Engineering Technology (IJRASET)
ISSN: 2321-9653; IC Value: 45.98; SJ Impact Factor: 6.887
Volume 6 Issue IV, April 2018- Available at www.ijraset.com

A Unified approach to the Load Flow Analysis of AC-DC Hybrid Distribution System

Konetikalva Kesavulu Reddy[1], Lokanadham Kathari[2]
[1]*PG Scholar,* [2] *Associate Professor Sri Venkateswara College of Engineering & Technology (Autonomous), Chittoor, INDIA,*

Abstract: ***A unified load flow (LF) model for AC-DC hybrid distribution systems (DSs) is proposed. The proposed model can be applied in hybrid DSs with mixed configurations for AC/DC buses and AC/DC lines. A new classification of DS buses is also introduced for LF analysis. For the optimal accommodation of all types of anticipated loads and DGs, both AC and DC, the belief is that future DSs should be hybrid systems that include AC and DC buses, AC and DC lines, and AC-DC converters. Such predictions underscore the need for the development of a unified AC-DC load flow (LF) model that can be used for the planning and operation of future hybrid DSs. A set of generic LF equations has been derived based on comprehensive analysis of the possible AC-DC hybrid system configurations. Three binary matrices, which are used as a means of describing the configuration of the AC and DC buses and lines, have been employed in the construction of the unified power equations. These matrices enable a single configuration at a time to be activated in the power equations. The proposed LF model is generic and can be used for both grid-connected and isolated hybrid DSs. The new model has been tested using several case studies of hybrid DSs that include different operational modes for the AC and DC distributed generators (DGs). As a means of evaluating the effectiveness and accuracy of the proposed model, the LF solution was compared to the solution produced by MATLAB/SIMULINK.***

Keywords: Load Flow Analysis, AC-DC Hybrid Distribution System, Voltage Source Converter (VSC), Distributed Generation.

I. INTRODUCTION

Recent developments and trends in the electric power consumption clearly indicate an increasing use of dc in end-user equipment. Computers, TVs, and other electronic-based apparatus use low-voltage dc obtained by means of a single-phase rectifier followed by a dc voltage regulator. In factories, the same input stage is used for process-control equipment, while directly-fed ac machines have been replaced by ac drives that include a two-stage conversion process. Electrical energy production from renewable sources is at dc (as in photovoltaic systems and fuel cells). By using dc for distribution systems it would thus be possible to skip one stage in the conversion in all these cases, with consequent savings and higher reliability due to a decreased number of components. Moreover, energy delivery at dc is characterized by lower losses and voltage drops in lines. The benefits of using DC power alongside AC power in DSs have been demonstrated in numerous research studies [4]– [9]. For example, the work reported in [4] revealed that the utilization of DC power in a distribution network improved the voltage profile and the power capacity of the network feeders. In [6]–[8], using DC power in a distribution network led to lower power losses than occur in a purely AC network. The authors of [9] introduced an AC-DC bilayer DS that avoids the overloading of secondary distribution transformers. Theload flow (LF) calculation for AC-DC hybrid power systems is performed using a sequential approach, in which the AC and DC LF equations are solved independently at each iteration until the boundary conditions of the AC-DC converters are satisfied. Because the sequential method is complicated and time-consuming. In the integrated method, both AC and DC LF equations are solved together at each iteration in order to overcome the drawbacks associated with the sequential method. In this type of analysis, the main hybrid grid is divided into several AC and DC sub grids that have to be solved iteratively until convergence is reached.

II. MODELING OF HYBRID AC/DC SYSTEM

The power system is modeled with differential and algebraic equations (DAE). The first order differential equations describe the dynamics of the system, while the algebraic equations arise from the assumption that fast variables have already reached their steady state on the time horizon of interest.In electro-mechanical simulation studies, voltages and currents in ac grids are represented by time-varying phasors ignoring fast electro-magnetic transients (EMT). In addition, symmetrical components are assumed and lumped parameters are used instead of distributed parameters, for example in transmission lines. Hybrid DSs consist of a variety of AC and DC components, including loads, generating units, lines, and buses. These components can be interconnected in different hybrid con- figurations. This section explains the classification of AC/DC buses and discusses the VSC steady-state model used in

©IJRASET (UGC Approved Journal): All Rights are Reserved

the proposed LF model. The proposed classification of the AC-DC hybrid configurations that was used for deriving the unified AC-DC power equations is also presented and analyzed.

A. Classification of AC and DC Buses

Hybrid DS buses can be either AC or DC. Hybrid DSs include DC loads and DC DGs alongside the conventional AC loads and AC generators. Examples of DC DGs include PV panels and fuel cells. EVs and modern elevators represent examples of DC loads. In the case of AC buses, AC-DC converters are necessary for connecting DC loads and DC DGs to an AC bus, as shown in Fig.1(a). The arrangement is reversed in the case of DC buses, as shown in Fig.1(b).

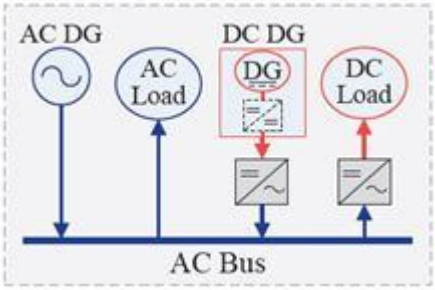

Fig.1(a) Connection of Loads and DGs to AC Bus

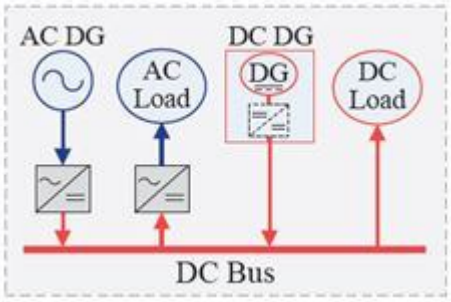

Fig .1(b) Connection of Loads and DGs to DC Bus

In the proposed LF model, AC buses are classified as follows:

1) AC slack (or reference) bus
2) AC load (or P-Q) bus
3) AC voltage-controlled (or P-V) bus
4) AC droop-based DG bus

B. AC-DC Converter Model

In this study, VSCs are installed in the network lines for ACDC power conversions. The DC side of the VSC is a unipolar circuit that has two DC lines, as shown in Fig. 2. The converter impedance Zc shown in Fig. 2 includes the elements connected between the point of common coupling (PCC) and the AC bus of the VSC, such as power transformers, phase reactors, or low pass filters. Since Zc is connected between two AC buses, it can be modeled.

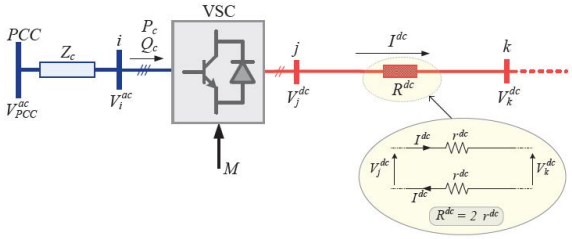

Fig. 2 Model of a voltage source converter

©IJRASET (UGC Approved Journal): All Rights are Reserved

The steady-state model of the VSC can be represented by the following equations. First, the AC-side voltage V ac i is related to the DC-side voltage V dc j as follows

$$V^{ac}{}_{i,LL_{rms}} = K_{vsc} M V^{ac}{}_{base} = K_{vsc} V^{dc}{}_{base} \quad (1)$$

Where M is the modulation index of the VSC. The value of the converter constant $K_{vsc}$is dependent on the type of the VSC as well as the type of the pulse width modulation (PWM) strategy. For the three-phase sinusoidal PWM converter used in this paper, the value of $K_{vsc}$is equal to (√3/2 √2)

The relation between the AC voltage base and the DC voltage base is given by

$$V^{ac}{}_{base} = K_{vsc} V^{dc}{}_{base} \quad (2)$$

Accordingly, a 1 p.u. AC voltage is equivalent to a 1 p.u. DC voltage at a unity modulation index, as expressed in

$$V^{ac}{}_{i.p.u.} = M V^{dc}{}_{j.p.u.} \quad (3)$$

The relation between the DC power and the AC active power is a function of the efficiency η_cf the converter, as follows:

$$P_c = {P_c^{dc}}/{\eta_c} = (V^{dc}{}_j I^{dc})/\eta_c \quad (4)$$

Where the I^{dc}DC current is given by

$$I^{dc} = G^{dc}(V^{dc}{}_j - V^{dc}{}_k) \quad (5)$$

Substituting (3) and (5) in (4) gives

$$P_c = \frac{G^{dc}{}_{p.u.}}{\eta_c}(M^{-2}(V^{ac}{}_{i.p.u.})^2 - M^{-1} V^{ac}{}_{i.p.u.} \quad (6)$$

The reactive power Qc at the AC side of the VSC can be either controlled using a direct set point or calculated as follows:

$$Q_c = P_c \tan\varphi_C \quad (7)$$

Regarding the operation of the VSC, two parameters need to be specified. The first parameter can be the AC active power, the DC power, the modulation index, or the DC-side voltage. The second parameter can be the converter reactive power, the AC-side voltage, or the power factor angle. For isolated DSs (e.g., AC-DC hybrid microgrids), the VSC can be controlled autonomously to achieve power sharing between the AC and DC sub grids without the need to specify the aforementioned two parameters. In this case, the frequency ω and the DC voltage V dc are used as loading indicators for the AC and DC sub grids, respectively. In order to equalize the loading of the AC and DC sub grids, the active power flow between the two sub grids can be determined using (8) [28]. The VSC in an isolated DS can also support the reactive power when the active power flows from the DC side to the AC side.The converter reactive power can then be controlled using the same reactive power drop of an AC DG (equation (28) in Section III) unless the capacity limit of the VSC is reached [24]. It should be noted that the upper and lower limits of the modulation index should be taken into consideration in order to avoid over modulation and excessive harmonics [14].

$$\hat{\omega} = \hat{V}^{dc} \quad (8)$$

$$\hat{\omega} = \frac{\omega - 0.5(\omega^{max} + \omega^{min})}{0.5(\omega^{max} - \omega^{min})} \quad (9)$$

$$\hat{V}^{dc} = \frac{V^{dc} - 0.5(V^{dc,max} + V^{dc,min})}{0.5(V^{dc,max} - V^{dc,min})} \quad (10)$$

©IJRASET (UGC Approved Journal): All Rights are Reserved

C. Classification of AC-DC Hybrid Configurations

This subsection presents a comprehensive analysis and proposed classification of the possible cases of AC-DC connections. AC/DC buses can be interconnected via AC/DC lines and AC-DC converters according to one of the following cases:

1) *Connection between Two AC Buses:* A connection between two AC buses can be achieved using the method exemplified by either Case 1 or Case 2. In Case 1, two AC buses are connected via an AC line, as shown in Fig. 3(a). In this case, the active and reactive power equations are given by

$$P^{(a)}{}_{nm} = V^2{}_n G_{nm} - V_n V_m (G_{nm} \cos\theta_{nm} + B_{nm} \sin\theta_{nm}) \quad (11)$$

$$Q^{(a)}{}_{nm} = -V^2{}_n B_{nm} - V_n V_m (G_{nm} \sin\theta_{nm} - B_{nm} \cos\theta_{nm}) \quad (12)$$

In Case 2, a DC line connects the two AC buses via two AC-DC converters, as shown in Fig. 3(b). The active and reactive power equations are expressed as equation (13) and (14), respectively. The values of a_1 and b_1, obtained from (15) and (16), respectively, are dependent on the direction of the power flow. If the power flows from bus n to bus m, the VSC at bus n functions as a rectifier, while the VSC at bus m functions as an inverter. In this case, the values of a_1 and b_1 become 1 and 0, respectively. In contrast, if the power flows from bus m to bus n, the values of a_1 and b_1 become 0 and 1, respectively.

$$P^{(b)}{}_{nm} = G^{dc}{}_{nm}(M^{-2}{}_n V^2{}_n - M^{-1}{}_{nm} V_n M^{-1}{}_{mn} V_m)\left(\frac{a_1}{\eta_{c-nm-r} + b_1 \eta_{c-nm-i}}\right) \quad (13)$$

$$Q^{(b)}{}_{nm} = P^{(b)}{}_{nm} \tan\varphi_{c-nm} \quad (14)$$

$$a_1 = 0.5(1 + sign(M^{-1}{}_{nm} V_n - M^{-1}{}_{mn} V_m)) \quad (15)$$

$$b_1 = 0.5(1 - sign(M^{-1}{}_{nm} V_n - M^{-1}{}_{mn} V_m)) \quad (16)$$

$$sign(x) = \begin{cases} 1 & if \quad x > 0, \\ -1 & if \quad x < 0, \\ 0 & if \quad x = 0, \end{cases} \quad (17)$$

2) *Connection between AC and DC Busses:* The connection between two different types of buses (Ac and DC) can be ac complished through the installation of a DC line and VSC. Since this case involves two different type of buses (Ac and DC), the formulation of the power flow equation at differ from one side that at the other side. Consideration of the following two cases facilities the formulation of the power flow equations as: 1) case 3a entailsthe studyof the power flow from the AC side, and 2) case 3b involves the examination of the power flow from the DC side. Case 3a and 3b are illustrated in fig.3(c) and fig.(d), respectively. In this case 3a, the power equations 3a and 3b are illustrated (18)-(21) for the AC bus are formulated in the same manner as in case 2.

$$P^{(c)}{}_{nm} = G^{dc}{}_{nm}(M^{-2}{}_n V^2{}_n - M^{-1}{}_{nm} V_n V_m)\left(\frac{a_2}{\eta_{c-nm-r} + b_2 \eta_{c-nm-i}}\right) \quad (18)$$

$$a_2 = 0.5(1 + sign(M^{-1}{}_{nm} V_n - V_m)) \quad (19)$$

$$b_1 = 0.5(1 - sign(M^{-1}{}_{nm} V_n - V_m)) \quad (20)$$

$$Q^{(c)}{}_{c-nm} = P^{(c)}{}_{nm} \tan\varphi_{c-nm} \quad (21)$$

©IJRASET (UGC Approved Journal): All Rights are Reserved

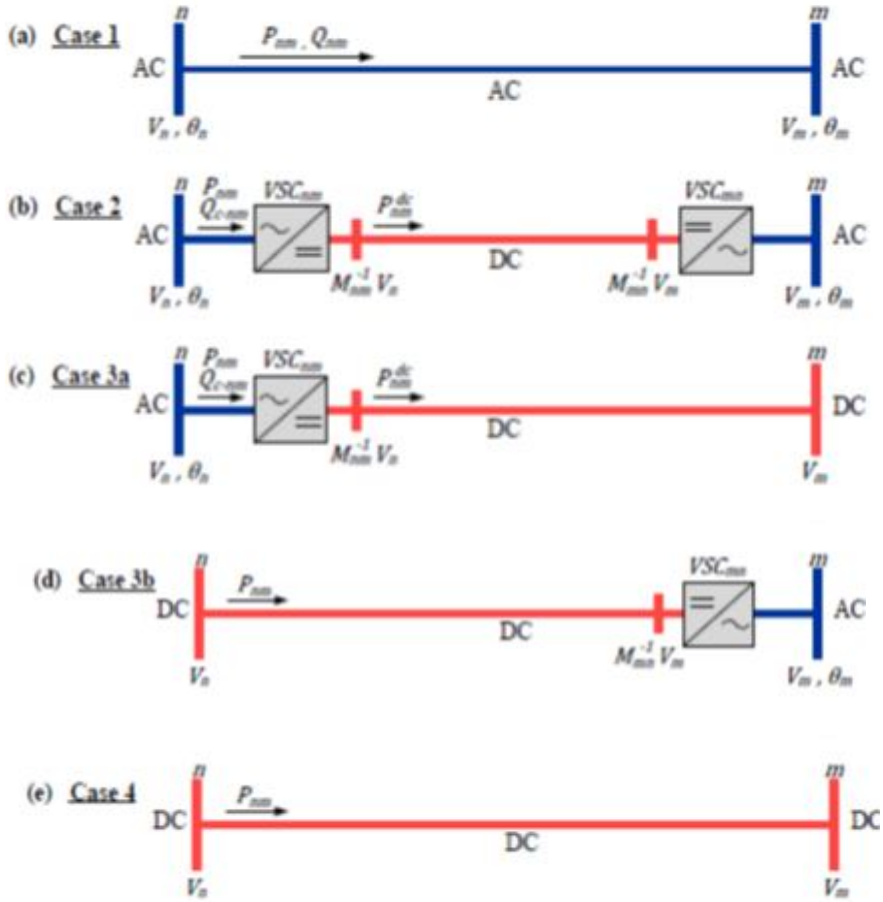

Fig.3 possible connection of AC-DC connections

For Case 3b, the power equation at the DC-bus side is expressed as follows:

$$P^{(d)}{}_{nm} = G^{dc}{}_{nm}(V^2{}_n - V_n M^{-1}{}_{nm} V_m) \quad (22)$$

3) *Connection between Two Dc Buses:* Case 4 represents a connection between two DC buses via a DC line , as depicted in Fig. 3(c). In this case, the DC power equation is given by

$$P^{(e)}{}_{nm} = G^{dc}{}_{nm}(V^2{}_n - V_n V_m) \quad (23)$$

III. FORMULATION OF THE UNIFIED LOAD FLOW(LF) MODEL

Implementation of the LF model in any generic hybrid DS requires that the system configuration and parameters be described in a matrix format. The following matrices have been defined and are used as input for the LF model.

A. *Configuration Matrices*

The following three binary matrices are defined based on the given hybrid DS configuration:

1) *Bus-type vector W (Nb×1):* It describes the type (AC or DC) of each bus in the hybrid DS network:

W_n= 1, if bus n is DC.
= 0, if bus n is AC.

B. *AC admittance matrix Y($N_b \times N_b$):*

The element Y_{nm}in this matrix is the admittance of the AC line connecting bus n to bus m, and can be expressed as follows:

©IJRASET (UGC Approved Journal): All Rights are Reserved

$$Y_{nm}(\omega) = G_{nm}(\omega) + jB_{nm}(\omega) = \frac{1}{R_{nm}+j\omega L_{nm}} \quad (24)$$

Where ($\omega = \omega * = 2\pi \times 60$ Hz) for grid-connected systems.

C. DC conductance matrix $G^{dc}(N_b \times N_b)$:

The element $G^{dc}{}_{nm}$ in this matrix is the conductance of the DC line connecting bus n to bus m.

D. Power Balance Equations

The unified active and reactive power balance equations for the AC-DC hybrid system are given by

$$P^{inj}{}_n = P^{cal}{}_n \quad , \quad \forall\, n = 1,2,\dots,N_b \quad (25)$$

$$Q^{inj}{}_n = Q^{cal}{}_n \quad , \quad \forall\, n = 1,2,\dots,N_b \quad (26)$$

The equations for $P^{inj}{}_n$, $P^{cal}{}_n$, $Q^{inj}{}_n$, and $Q^{cal}{}_n$, respectively. $P^{inj}{}_n$, and $Q^{inj}{}_n$ represent the net active and reactive power injected into bus n and are dependent on the loads and DGs connected at that bus. The respective equations for $P^{inj}{}_n$, and $Q^{inj}{}_n$, , are derived based on the AC and DC buses classified as indicated in Fig.1.1. $P^{cal}{}_n$ And $Q^{cal}{}_n$ represent the calculated active and reactive power transmitted through the lines connected to bus n. The respective equations for $P^{cal}{}_n$ and $Q^{cal}{}_n$, are derived based on hybrid configuration cases classified according to Section II-C, and The configuration matrices (W, U, and D). For a given set of elements for the matrices (W, U, and D), only one configuration is activated at a time in the power equations. For isolated AC-DC hybrid DSs, the droop-based control can be used to achieve proportional power sharing for AC and DC DGs [28]. In this case, the AC droop equations (27)-(28) as well as the DC droop equation (29).

$$P^{ac}{}_G = (\omega_0 - \omega)/\psi^{ac}{}_p \quad (27)$$

$$Q^{ac}{}_G = (V^{ac}{}_0 - V^{ac})/\psi^{ac}{}_q \quad (28)$$

$$P^{dc}{}_G = (V^{dc}{}_0 - V^{dc})/\psi^{dc}{}_q \quad (29)$$

Where

$$\psi^{ac}{}_p = (\omega^{max} - \omega^{min})/P^{ac,max}{}_G \quad (30)$$

$$\psi^{ac}{}_q = (V^{ac,max} - V^{ac,min})/Q^{ac,max}{}_G \quad (31)$$

$$\psi^{dc}{}_q = (V^{dc,max} - V^{dc,min})/P^{dc,max}{}_G \quad (32)$$

E. Parameters and Variables for AC and DC Buses

Table I summarizes the known parameters and unknown variables for all types of system buses. The known parameters at each bus are considered to be equality constraints, while the unknown variables constitute the output of the LF model.

F. Solution Procedures

The hybrid LF problem is defined by a system of equations that are solved simultaneously. In order to find the LF solution in this study, a generalized reduced gradient (GRG) method [31] is used for solving the optimization problem descry bed below

$$\text{Min } \|F(x)\|_2 \quad , \quad x \in \mathbb{R}^{n_v} \quad (33)$$

Where

©IJRASET (UGC Approved Journal): All Rights are Reserved

$$F(x) = \begin{cases} P^{inj}{}_i - P^{cal}{}_i & ,\forall\, i \in N_b \\ Q^{inj}{}_i - Q^{cal}{}_i & ,\forall\, i \in N_b \\ P^{ac}{}_{Gi} - \frac{1}{\psi^{ac}{}_{p,i}}(\omega_0 - \omega) & ,\forall\, i \in N^{ac}{}_{G-dr} \\ Q^{ac}{}_{Gi} - \frac{1}{\psi^{ac}{}_{q,i}}\left(V^{ac}{}_{i,0} - V^{ac}{}_i\right) & ,\forall\, i \in N^{ac}{}_{G-dr} \\ P^{dc}{}_{Gi} - \frac{1}{\psi^{dc}{}_{p,i}}\left(V^{dc}{}_{i,0} - V^{dc}{}_i\right) & ,\forall\, i \in N^{dc}{}_{G-dr} \\ \hat{V}^{dc}{}_i - \hat{\omega} & ,\forall\, i \in N_{c-iso} \\ Q_{c-i} - \frac{1}{\psi^{ac}{}_{q,c-i}}\left(V^{ac}{}_{c-i,0} - V^{ac}{}_{c-i}\right), & ,\forall\, i \in N_{c-iso} \end{cases} \quad .. (34)$$

F(x) is the set of the system equations that include the power balance equations, the droop equations, and the VSC equations; ($N^{ac}{}_{G-dr}$ and $N^{dc}{}_{G-dr}$) are the number of the droop based AC and DC DGs, N_{c-iso}respectively; is the number of VSCs in an isolated DS; and nv is the number of the system unknown variables x. The first step in the solution procedures is to define the type, the given parameters, and the unknown variables for each bus in the hybrid DS, as presented in Table I. In the second step, the configuration matrices (W, U, and D) as well as the AC admittance matrix Y and the DC conductance matrix $G^{dc}$are constructed. In the third step, the system parameters are converted to per-unit values, and a flat start (V (0) = 1.0 p.u. and θ (0) = 0.0 ◦) is assumed for the unknown system voltages. Finally, the data prepared in the previous steps are then used as input to the LF model.

IV. MATLAB RESULTS

The case studies that were used for evaluating the effectiveness and accuracy of the proposed load flow(LF) model. In the case studies, the proposed LF model was implemented in a general algebraic modeling system (GAMS) and executed. In the first case study, the accuracy of the proposed model was verified against the steady-state solution produced by MATLAB/SIMULINK. The MATLAB/SIMULINK is a time-domain software that can accurately model power system components using differential equations, and thus can be used for validating LF algorithms. Such software takes a huge amount of computational time compared to the algebraic LF methods that can perform steady-state analyses in very short time.

A. Modified IEEE 33-Bus Test System

The modified IEEE 33-bus DS was used for the second case study, as shown in Fig.4 The network impedances and the load data are listed in Table 1 and Table 2, respectively. The base values used for this test system are s_{base} = 10 MVA, $V^{ac}{}_{base}$= 12.66 kV, ω ∗= 2π×60 Hz, and $V^{dc}{}_{base}$= 20.67 Kv

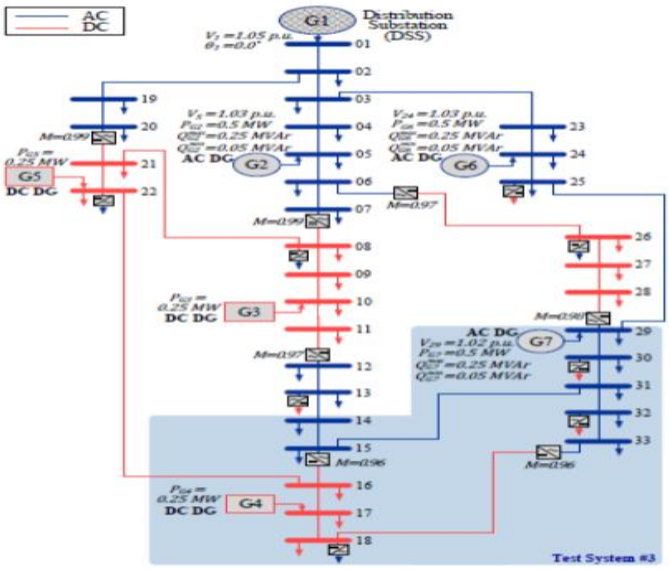

Fig.4. 33-Bus Hybrid Distribution System.

Table1: Impedance of the 33-bus Test system (ω = 1.0 P.U.)

From Bus	To Bus	Resistance (Ω)	Reactance (Ω)
1	2	0.0922	0.0470
2	3	0.4930	0.2511
2	19	0.1640	0.1565
3	4	0.3660	0.1864
3	23	0.4512	0.3083
4	5	0.3811	0.1941
5	6	0.8190	0.7070
6	7	0.1872	0.6188
6	26	0.4060*	-
7	8	1.4228*	-
8	9	2.0600*	-
8	21	4.0000*	-
9	10	2.0880*	-
10	11	0.3932*	-
11	12	0.7488*	-
12	13	1.4680	1.1550
13	14	0.5416	0.7129
14	15	0.5910	0.5260
15	16	1.4926*	-
15	31	2.0000	2.0000
16	17	2.5780*	-
16	22	4.0000*	-
17	18	1.4640*	-
18	33	1.0000*	-
19	20	1.5042	1.3554
20	21	0.8190*	-
21	22	1.4178*	-
23	24	0.8980	0.7091
24	25	0.8960	0.7011
25	29	0.5000	0.5000
26	27	0.5684*	-
27	28	2.1180*	-
28	29	1.6084*	-
29	30	0.5075	0.2585
30	31	0.9744	0.9630
31	32	0.3105	0.3619
32	33	0.3410	0.5302

Table 2: Load Data of The 33-Bus Test System

Bus No.	P_L^{ac}	Q_L^{ac}	P_L^{dc}
1	-	-	-
2	200	120	-
3	180	80	-
4	240	160	-
5	125	60	-
6	200	100	-
7	200	100	-
8	120	70	120
9	-	-	120
10	-	-	120
11	-	-	300
12	120	70	-
13	60	15	60
14	400	200	-
15	260	105	-
16	-	-	60
17	-	-	60
18	45	20	45
19	180	80	-
20	180	80	-
21	-	-	300
22	90	45	90
23	180	100	-
24	115	60	-
25	300	100	300
26	60	35	60
27	-	-	200
28	-	-	120
29	85	35	-
30	100	60	100
31	170	50	-
32	145	70	145
33	240	160	-

©IJRASET (UGC Approved Journal): All Rights are Reserved

Table 3: Line Flow solution for the 33-Bus Test system

Bus No.	V_n (p.u)	θ_n (deg.)
1	1.05000	0.00000
2	1.04709	-0.00972
3	1.03776	-0.02781
4	1.03360	-0.03683
5	1.03000	-0.05114
6	1.01912	-0.27694
7	1.01869	-0.29890
8	1.02923	-
9	1.02674	-
10	1.02479	-
11	1.02430	-

Bus No.	V_n (p.u)	θ_n (deg.)
12	0.99317	-0.62317
13	0.99215	-0.66568
14	0.99225	-0.66363
15	0.99449	-0.62944
16	1.03692	-
17	1.03884	-
18	1.03930	-
19	1.04503	-0.05930
20	1.02871	-0.43950
21	1.03702	-
22	1.03715	-

Bus No	V_n (p.u)	θ_n (deg.)
23	1.03477	-0.05338
24	1.03000	-0.11852
25	1.02238	-0.21870
26	1.04951	-
27	1.04808	-
28	1.04371	-
29	1.02000	-0.22492
30	1.01404	-0.24914
31	1.00228	-0.50558
32	1.00006	-0.57217
33	0.99823	-0.63485

V. SIMULATION RESULTS

Comparision of Normal,proposed and with Limited DG's

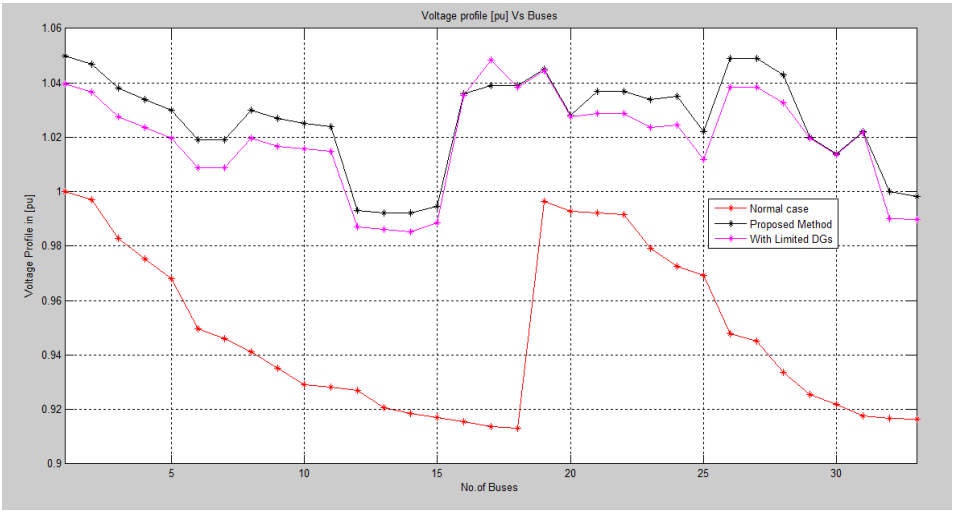

Fig.5 Voltage Profile(p.u) vs Buses

The results obtained from the proposed LF model are listed in Tables. The LF model converged with a system total power mismatch of 1.2×10-10 p.u., and the computational time was found to be 207 ms. The above fig(5) shows the simulation results for normal, proposed and with limited DGs of voltage profile vs buses.

A. Isolated AC-DC Hybrid Test System

For the third case study, it is assumed that the shaded area (Test System # 3) in Fig. 4 has been islanded. Two more DGs were added to this isolated system:

1) AC DG at bus 31
2) DC DG at bus 16.

©IJRASET (UGC Approved Journal): All Rights are Reserved

The two AC DGs as well as the two DC DGs are operated as droop-controlled DGs. Because the system frequency is considered as an additional variable, the voltage angle of one of the system AC buses (e.g., bus 31) is taken as a reference in order to equalize the number of variables and the number of system equations. Taking the limits of the frequency and the AC/DC voltages as ± 1% and ± 5%, respectively. The upper and lower limits of the modulation index are given as 1.0 and 0.77, respectively. and the modulation indices of the VSCs were found to be M_{15-16}= 0.991 and M_{33-18}= 0.996. The LF model converged with a system total power mismatch of 0.9×10^{-10}p.u., and the computational time was found to be 167 ms.

VI. CONCLUSION

A novel AC-DC LF model for hybrid DSs. The detailed analysis presented includes consideration of the possible AC-DC hybrid DS configurations. In the proposed LF model, VSCs are employed for AC-DC power conversions. The proposed model can solve the LF problem for the AC and DC portions of the hybrid DS simultaneously based on the integration of the AC and DC power equations into one unified model. Employing three binary matrices in the unified power equations allows any configuration of AC-DC hybrid DSs to be described, which introduces a high degree of flexibility into the proposed LF model. The proposed model was applied for solving the LF problem of grid-connected and isolated hybrid DSs that included a variety of types of loads, DGs, buses, and lines. The effectiveness of the proposed model was verified against the steady-state solution produced by MATLAB/SIMULINK. The results demonstrate that the proposed LF model can provide an accurate solution while also offering the flexibility and speed required for online smart-grid applications.

REFERENCES

[1] European Photovoltaic Industry Association (EPIA). (2015, May). Global market outlook for photovoltaics 2014-2018.
[2] International Renewable Energy Agency (IRENA). (2015, May). Battery storage for renewables: market status and technology outlook, 2015.
[3] Energy Agency (IEA). (2015, April). Global EV outlook 2015.
[4] K. Chaudhary, J. M. Guerrero, and R. Teodorescu, "Enhancing the capacity of the AC distribution system using DC interlinks–A step toward future DC grid," IEEE Trans. Smart Grid, vol. 6, no. 4, pp.1722–1729, July 2015.
[5] K. Kurohane, T. Senjyu, A. Yona, N. Urasaki, T. Goya, and T. Funabashi, "A hybrid smart AC/DC power system," IEEE Trans. Smart Grid, vol. 1, no. 2, pp. 199–204, Sept 2010.
[6] M. Starke, L. M. Tolbert, and B. Ozpineci, "AC vs. DC distribution: A loss comparison," Transmission and Distribution Exposition Conference: IEEE PES Powering Toward the Future, PIMS, 2008.
[7] T. Kaipia, P. Salonen, J. Lassila, and J. Partanen, "Possibilities of the low voltage DC distribution systems," Nordac, Nordic Distribution and Asset Management Conference, pp. 1–10, 2006
[8] T. Kaipia, P. Salonen, J. Lassila, and J. Partanen, "Application of low voltage DC distribution system, a techno-economical study," 19th International Conference on Electricity Distribution, Vienna, no. 0464, pp. 21–24, 2007.

©IJRASET (UGC Approved Journal): All Rights are Reserved

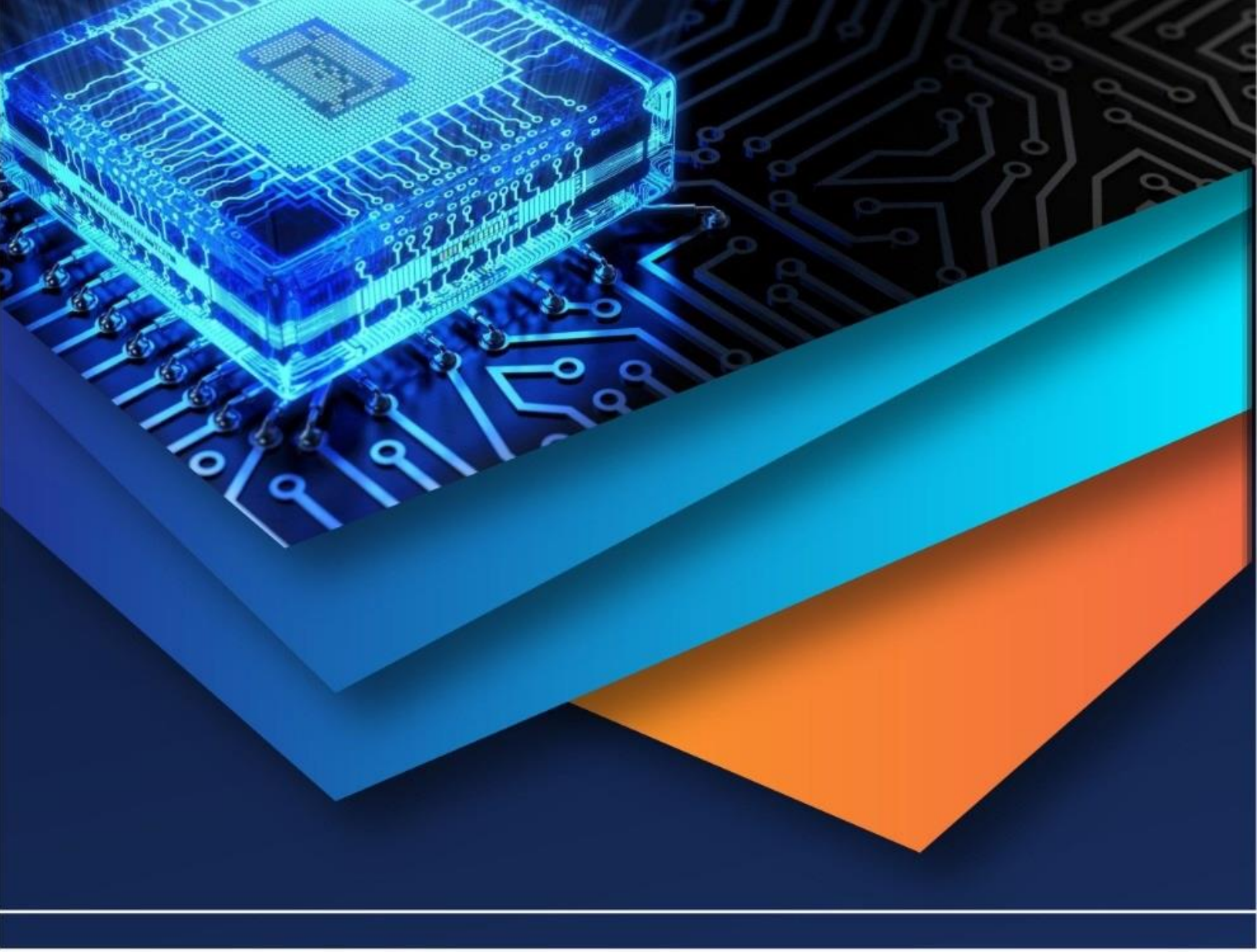

10.22214/IJRASET

45.98

IMPACT FACTOR: 7.129

IMPACT FACTOR: 7.429

INTERNATIONAL JOURNAL FOR RESEARCH

IN APPLIED SCIENCE & ENGINEERING TECHNOLOGY

Call : 08813907089 (24*7 Support on Whatsapp)